Available online at www.sciencedirect.com

ScienceDirect

Procedia Engineering 100 (2015) 746 – 755

Procedia Engineering

www.elsevier.com/locate/procedia

25th DAAAM International Symposium on Intelligent Manufacturing and Automation, DAAAM 2014

Stiffness Analysis of Wood Chair Frame

Seid Hajdarević*, Ibrahim Busuladžić

University of Sarajevo, Mechanical Engineering Faculty, Vilsonovo šetalište 9, Sarajevo 71000, Bosnia and Herzegovina

Abstract

This paper presents a stiffness analysis of a statically indeterminate wood-chair side-frame. Numerical calculations are carried out with a 'linear elastic model' for orthotropic materials. The mathematical model is solved by a 'finite element method'. The matrix analysis of structure is carried out by a 'direct stiffness method'. The frame joints are assumed to be ideally rigid and also as semi-rigid. Horizontal displacement of the top point of the back post is calculated for the most frequently used type of loading for the structure. The results of the calculation indicate that chair side frame becomes stiffer as the position of the stretcher is lowered and/or the stretcher cross section is increased. The results revealed that stiffness of joints in a frame had a considerable impact on the structure deflection. A satisfactory agreement was found between the numerical results and the results obtained by direct stiffness method.

Peer-review under responsibility of DAAAM International Vienna

Keywords: wood; chair; joint; stiffness; FEM; direct stiffness method

1. Introduction

In the common structural analysis of a construction, structural behavior for even a simple frame is calculated by considering certain idealizations. Joints are assumed to be ideally rigid or pinned. In most structures, joints are one of the most important components and their significant effect on the structure's behavior could not be ignored in the analysis. Structures analysis using the realistic joint behavior (`semi-rigid joint`) has become an integral part of the design process of the construction industry. Development of technologies and materials has created a need to introduce this approach in furniture construction design.

* Corresponding author. Tel.: +387-33-729-824; fax: +387-33-653-055.
E-mail address: hajdarevic@mef.unsa.ba

Peer-review under responsibility of DAAAM International Vienna
doi:10.1016/j.proeng.2015.01.428

Framed structure represents the most widely used type of furniture constructions. Common furniture frames are structurally complex, manufactured by connecting members with shape-adhesive joints and normally made from wood. Attempts are being made to find applicable methods and solutions that would improve the design process of wooden-frame structures. The analytical models applied so far, are usually limited to solve statically indeterminate problems and provide an approximate preview of a structure's behavior. The significant effect of joint properties on the distribution of internal force in the structure has been neglected by the approach to separate design of members and joints. The literature studied has established that investigations are focused on the numerical methods of furniture analysis. Eckelman introduced the semi-rigid joint concept into furniture analysis by the semi-rigid connection factor. He has shown that the magnitude of the force at any point is a function of the stiffness of essentially all of the members and joints in the frame [1]. Later, authors considered stiffness as design tool and observed different joint properties with different effects in the structure [2]. Numerical methods, such as the 'finite element method', are applicable and effective for the analysis of real wood structures [3, 4]. The limitations of numerical analysis are the complexity of numerical models related to the orthotropic properties of the applied materials and complexity of network geometry. As design and optimization of structure have been largely related to the design of the joint, an attempt has been made to replace whole structure analysis with the consideration of critical structural points (joint) only [5, 6, 7, 8, 9].

2. Research objective and methodology

The aim of this study was to determine stiffness of the wood structure, calculated by different methods and to compare the results in order to determine the effects of method, assumptions and simplifications used in the calculation of the results of a structure's stiffness. The objective was to make transparent what results are to be expected, depending on what approach to structural design was taken.

This study employed a numerical method (FEM) and the matrix analyses (Direct stiffness method) for the analysis of the stiffness of the frames of wooden furniture. The effects of the structural member and joint properties on the behavior of statically indeterminate physical model of wood-furniture construction used in this study were determined. The results obtained on the stiffness were compared in order to describe the influence of the frame stretcher cross-section dimensions and position, and joints properties on the stiffness of wooden constructions.

2.1. Mathematical model

The equation of momentum balance, expressed in the Cartesian tensor notation [10]

$$\int_S \sigma_{ij} n_j dS + \int_V f_i dV = 0 \tag{1}$$

and of the constitutive relation for the elastic material

$$\sigma_{ij} = C_{ijkl}\varepsilon_{kl} = \frac{1}{2} C_{ijkl}\left(\frac{\partial u_k}{\partial x_l} + \frac{\partial u_l}{\partial x_k}\right) \tag{2}$$

describe the stress and strain of a loaded solid body in static equilibrium. In the equations above, x_j are Cartesian spatial coordinates, V is the volume of solution domain bounded by the surface S, σ_{ij} is the stress tensor, n_j is the outward unit normal to the surface S, f_i is the volume force, C_{ijkl} is the elastic constant tensor components, ε_{kl} is the strain tensor, and u_k represents the point displacement. Twelve non-zero orthotropic elastic constants A_{ij} are related to the Young's modulus E_i, the Poisson's ratio ν_{ij}, and the shear modulus G_{ij}.

In order to complete the mathematical model, the boundary conditions have to be specified. The surface traction f_{Si} and/or the displacement u_S at the domain boundaries are known, i.e.

$$\sigma_{ij} n_j = f_{S_i} \quad \text{and} \quad u_i = u_S . \tag{3}$$

Governing equations (1) combined with the constitutive relations (2) are solved a numerical method based on the finite element. Calculations were performed by using the Catia software package.

2.2. Physical model

A chair with stretchers was selected for investigation. Since both the chair and the load are symmetric, two-dimensional analysis of chair side frame was sufficient. In figure 1, a vertical force F=600 N is applied to the top of the front leg and a horizontal force F_1=300 N acts on the top of the back post. The frame with the stretcher is loaded in a manner which corresponds to the load when chair is tilted backwards. This type of load causes a high value of bending force to act on the side rail to back post joint, (point B; Fig. 1.).

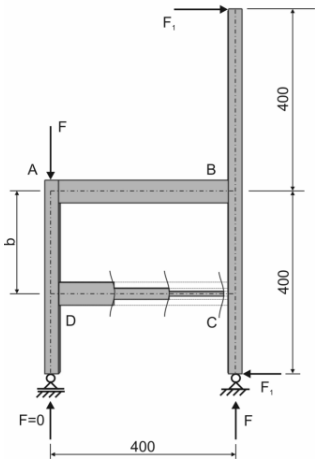

Fig. 1. Chair side frame - static scheme and dimensions.

Table 1. Cross section dimensions of the frame members.

No.	Members	Thickness (*mm*)	Width (*mm*)
1	Side rail	25,4	50,8
2	Stretcher	25,4; 15; 10	50,8; 25; 15
3	Back post	25,4	30
4	Back leg	25,4	30
5	Front leg	25,4	30

Geometries and measurements of the chair side frame are shown in Fig. 1. and Tab. 1. All variables except the stretcher cross section and distance between stretcher and side rail were held constant. Investigations were conducted on the side frames with three different dimensions of the stretcher cross section (thickness x width=25,4x50,8; 15x25; 10x15 mm) and five distance between stretcher and side rail (b=60; 100; 200; 300 and 350 mm).

Three numerical examples of chair's side-frame were analysed, Fig 2. The constitutive relation for the orthotropic material is used in the first and second example, Fig. 2 (a) and (b), and for isotropic material in the last example, Fig. 2 (c). Calculation was carried out for maple wood (*Acer saccharum Marsh.*). Its elastic properties, for wood

density ρ=0,57 g/cm^3 and moisture content of 12%, are presented in Tab. 2 [11]. Selected elastic properties of the isotropic material are E_L=13,81 GPa (longitudinal elastic modulus of maple) and ν=0,3.

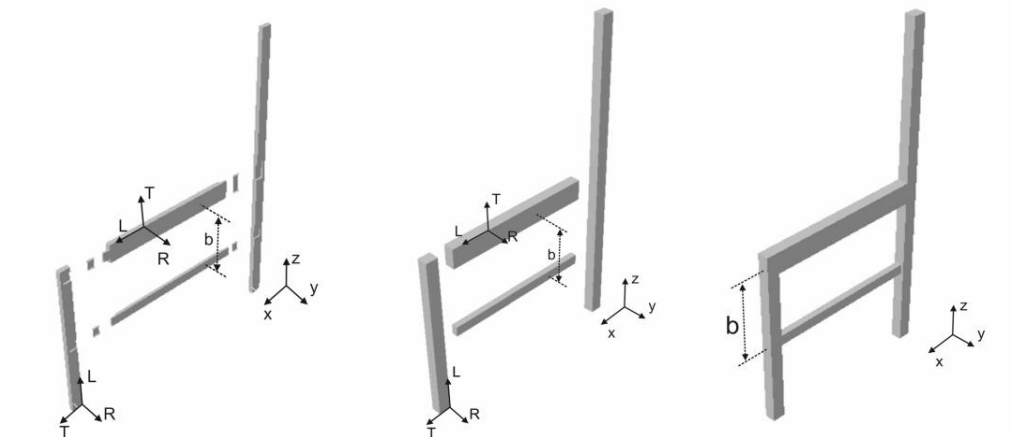

(a) (b) (c)

Fig. 2. Model: a) orthotropic with joints and symmetry plane, b) orthotropic and c) isotropic.

Table 2. Elastic properties of maple (*Acer saccharum Marsh.*).

Modulus of elasticity (*GPa*)			Rigidity modulus (*GPa*)			Poisson´s ratio					
E_L	E_R	E_T	G_{LR}	G_{LT}	G_{RT}	ν_{LR}	ν_{LT}	ν_{RT}	ν_{TR}	ν_{RL}	ν_{TL}
13,810	1,311	0,678	1,013	0,753	0,255	0,46	0,50	0,82	0,42	0,044	0,025

In the first example, rectangular mortise and tenon joints were selected for connecting frame members. Geometries and measurements of the tenon are shown in Tab. 3. A 0,1 mm thick gap was placed between the tenon and the mortise in which a glue bond was formed. The selected elastic properties of the polyvinyl acetate (PVAC) glue are *E*=465,74 MPa and ν=0,29 [6]. The shoulder of the tenon was contact-connected to the wall of the mortise. In another two numerical examples was introduced certain assumption. Frame joints were not modeled.

Table 3. Mortise and tenon joint measurements.

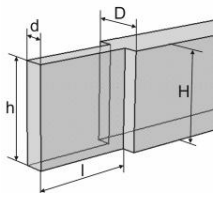

	Side rail - tenon dimensions (*mm*)						Rotational stiffness
Joint		*H*	*D*	*h*	*d*	*l*	(*Nm/rad*)
A		50,8	25,4	25,4	9,5	19,05	8906,03
B		50,8	25,4	50,8	9,5	19,05	20837,17
	Stretcher - tenon dimensions (*mm*)						Rotational stiffness
Joint: C, D		*H*	*D*	*h*	*d*	*l*	(*Nm/rad*)
	I	50,8	25,4	50,8	9,5	19,05	20837,17
case	II	25	15	25	7,5	19,05	5555,55
	III	20	10	20	10	19,05	3569,09

2.3. The matrix analyses of structure – Direct stiffness method

The direct stiffness method is intended to establish the total structure stiffness matrix **K** to relate the nodal force and displacement. The general expression is:

$$\begin{Bmatrix} R \\ \dots \\ X \end{Bmatrix} = \begin{bmatrix} K_{RR} & \vdots & K_{RX} \\ \dots & \vdots & \dots \\ K_{XR} & \vdots & K_{XX} \end{bmatrix} \begin{Bmatrix} r_R \\ \dots \\ r_X \end{Bmatrix} \tag{4}$$

where the unknown nodal displacement $\mathbf{r}_R$ corresponding to known nodal force **R** and the known nodal displacement $\mathbf{r}_X$ corresponding to unknown nodal forces **X**, Fig. 3(a).

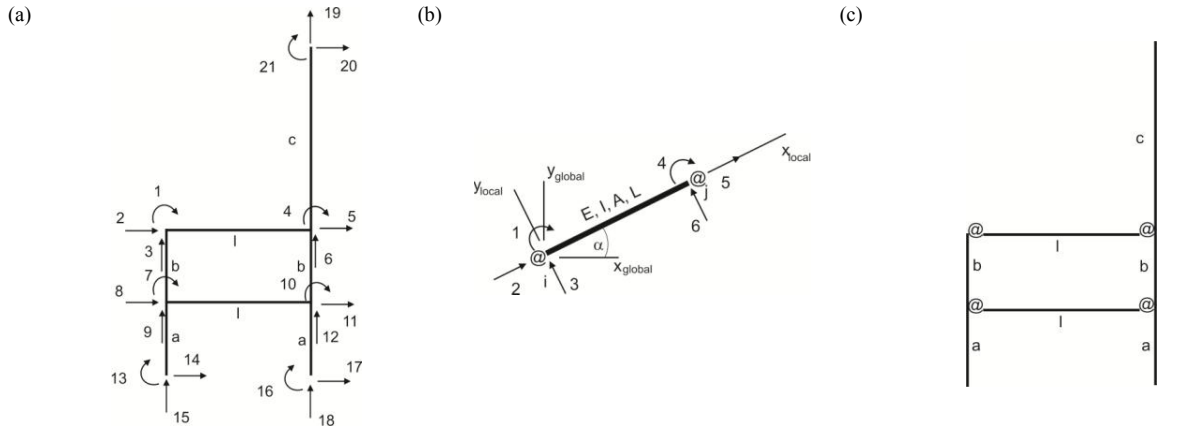

Fig. 3. Direct stiffness method: a) numbering of nodal displacements and forces, b) structural member with local and global coordinates, c) schematic representation of rotational end springs.

The total stiffness of the structure is constructed by superimposing the stiffness matrices of the individual structural members in global coordinates. The structure's stiffness coefficients are

$$K_{ik} = \sum_m \bar{k}_{ik}^m \tag{5}$$

where the summation extends over all m members meeting at node i and $\bar{k}_{ik}$ are the member stiffness coefficients in global coordinates. Transformation of the member stiffness matrix in local to global coordinates

$$\bar{\boldsymbol{k}} = \boldsymbol{a}^T \boldsymbol{k} \boldsymbol{a} \tag{6}$$

where **a** is the transformation matrix and **k** is the member stiffness matrix in local coordinates, Fig. 3(b) [12, 13].

The effects of semi-rigid joint at the ends of a member are incorporated in the analysis by modifying the stiffness matrix of the member

$$\boldsymbol{k}_m = \begin{bmatrix} \frac{4EI}{L}\theta_4 & & & & \\ \frac{2EI}{L}\theta_5 & \frac{4EI}{L}\theta_6 & & & \\ -\frac{6EI}{L^2}\theta_2 & -\frac{6EI}{L^2}\theta_3 & \frac{12EI}{L^3}\theta_1 & & \\ \frac{6EI}{L^2}\theta_2 & \frac{6EI}{L^2}\theta_3 & -\frac{12EI}{L^3}\theta_1 & \frac{12EI}{L^3}\theta_1 & \\ 0 & 0 & 0 & 0 & \frac{EA}{L} \\ 0 & 0 & 0 & 0 & -\frac{EA}{L} \quad \frac{EA}{L} \end{bmatrix} \tag{7}$$

where E is the modulus of elasticity, I is moment of inertia, A is cross sectional area and L is length of structure member. The parameters θ_i are

$$\theta_1 = \frac{r_i + r_j + r_{ij}}{3}, \quad \theta_2 = \frac{2r_i + r_{ij}}{3}, \quad \theta_3 = \frac{2r_j + r_{ij}}{3}, \quad \theta_4 = r_i, \quad \theta_5 = r_{ij}, \quad \theta_6 = r_j \tag{8}$$

The correction factors r_i, r_j and r_{ij} are

$$r_i = \frac{3\nu_i}{4-\nu_i\nu_j}, \quad r_j = \frac{3\nu_j}{4-\nu_i\nu_j}, \quad r_{ij} = \frac{3\nu_i\nu_j}{4-\nu_i\nu_j} \tag{9}$$

where ν_i and ν_j are the fixity factors [14]. The two dimensionless parameters are below

$$\nu_i = \frac{L}{L+\frac{3EI}{R_i}}, \quad \nu_j = \frac{L}{L+\frac{3EI}{R_j}} \tag{10}$$

These represent the semi-rigid connection as a percentage. The values of ν depend on the rotational stiffness R at the respective ends of the member and on its geometric and elastic properties.

Geometries, measurements and the loading diagram of the chair side frame were the same as in numerical analysis, see Fig. 1. The distance between stretcher and side rail is varied from 60 mm to 370 mm. Selected elastic properties of the material are E_L=13,81 GPa (longitudinal elastic modulus of maple). In the first case, joints are assumed to be ideally rigid and value of the fixity factor was $\nu = 1$. In the second case, the connections are assigned as semi-rigid, Fig. 3(c). The rotational stiffness value at the ends of side rail and stretcher are presented in Tab. 2. Description of the numerical and experimental determination of the rotational stiffness be found in [15, 16]. Calculations were performed by using the Matlab software package.

3. Results

The results of the numerical calculation, comprising of the translation displacement magnitude of the chair side frame with a stretcher cross section 15x25 mm and the distance between stretcher and side rail b=300 mm are shown in Fig. 4. As was expected, the analysis of the orthotropic model (with and without joints) and isotropic model revealed that the largest displacement occurs at the top points of the back post and a maximum stiffness has an isotropic model of frame. The effects of the orthotropic properties of wood and joints on the frame's stiffness are evident. Minimum stiffness or a maximum deformation has an orthotropic model of frame with joints as a result of the interaction between elements of the joints.

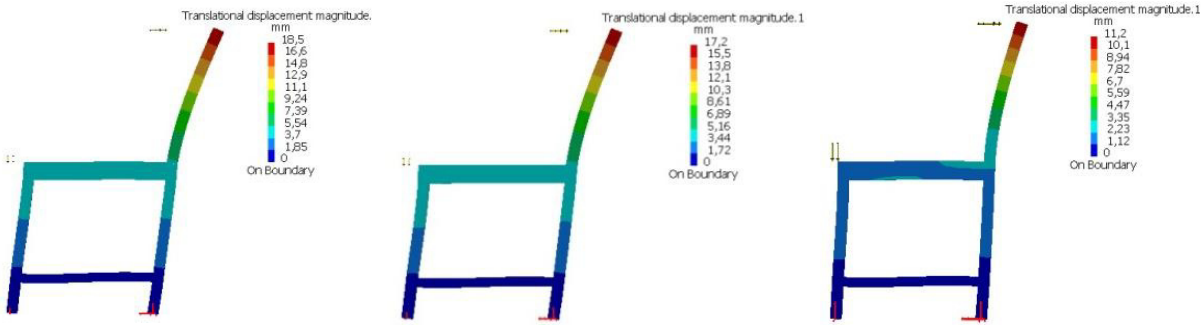

(a) (b) (c)

Fig. 4. Translation displacement: (a) orthotropic model with joints, (b) orthotropic model without joints, (c) isotropic model (scale 20:1).

The results of the matrix and numerical analyses of the structure, comprising of horizontal displacement for six points/nodes of the chair side frame, with a stretcher cross section 15x25 mm are given in Tab. 4. The stiffness of the frame is significantly lower if the joint's properties are included in the structural analysis.

The effect of the stretcher position and stretcher cross-section on the change of horizontal displacement of the top point of the back post for all computational cases was assessed. The position of the selected point is shown in Fig. 5(a) and a numerical example of frame deformations is presented in Fig. 5(b). Displacements of the top point of the back post for three cross section size of stretcher are shown in Fig. 6, 7, and 8.

Table 4. Horizontal displacement of frame points/nodes (10^{-3} *m*).

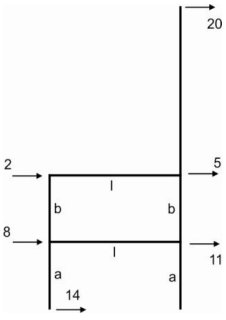

Method (model)	b (*cm*)	Node/point 2	5	8	11	14	20
FEM (isotropic)	10	5,65	5,66	5,30	5,32	4,3	14,2
	20	3,26	3,26	2,43	2,39	1,46	12,0
	30	2,23	2,23	0,773	0,745	0,216	11,2
Direct stiffness method (rigid joints)	10	5,9491	5,9706	5,6148	5,5409	4,3924	15,2454
	20	3,5039	3,5139	2,5839	2,5495	1,5298	12,9031
	30	2,4324	2,4386	0,8220	0,8010	0,2383	12,0082
FEM (orthotropic + joints)	10	9,61	9,65	8,61	8,58	5,96	23
	20	6,53	6,58	4,24	4,22	2,12	19,6
	30	5,2	5,23	1,53	1,51	0,4	18,5
Direct stiffness method (semi-rigid joints)	10	8,3729	8,3929	7,4172	7,3482	4,4599	20,1234
	20	5,8620	5,8717	3,7456	3,7121	1,5802	17,6724
	30	4,7154	4,7215	1,3646	1,3435	0,2390	16,7698

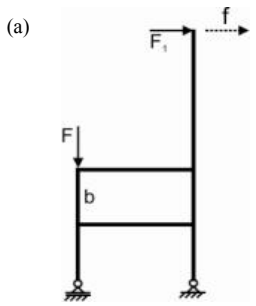

Fig. 5. (a) Horizontal displacement of the top point of the back post, (b) Deformations of the orthotropic model with joints (symmetry plane; scale 20:1).

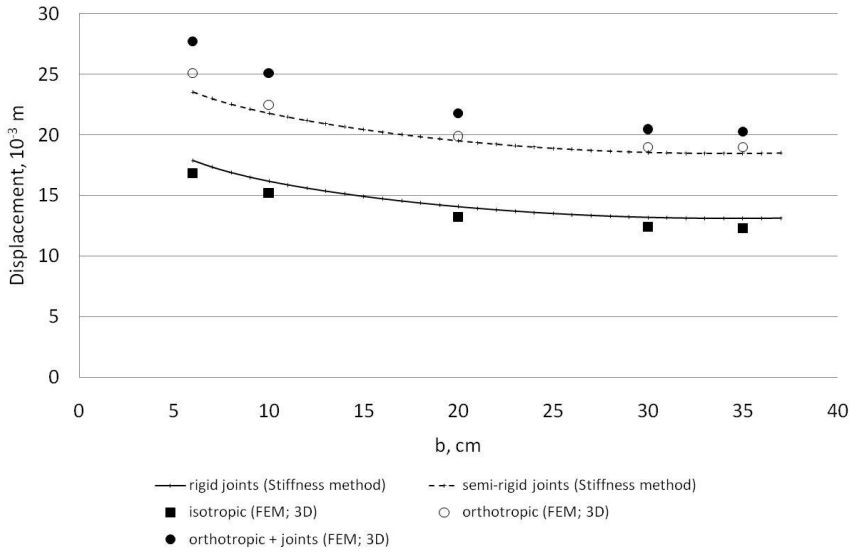

Fig. 6. Horizontal displacement of the frame top point – stretcher cross section 10x20 mm.

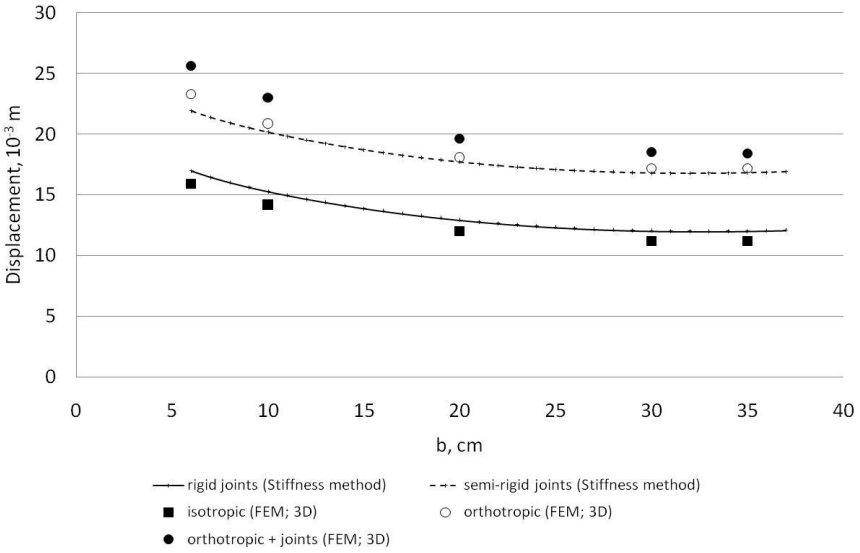

Fig. 7. Horizontal displacement of the frame top point – stretcher cross section 15x25 mm.

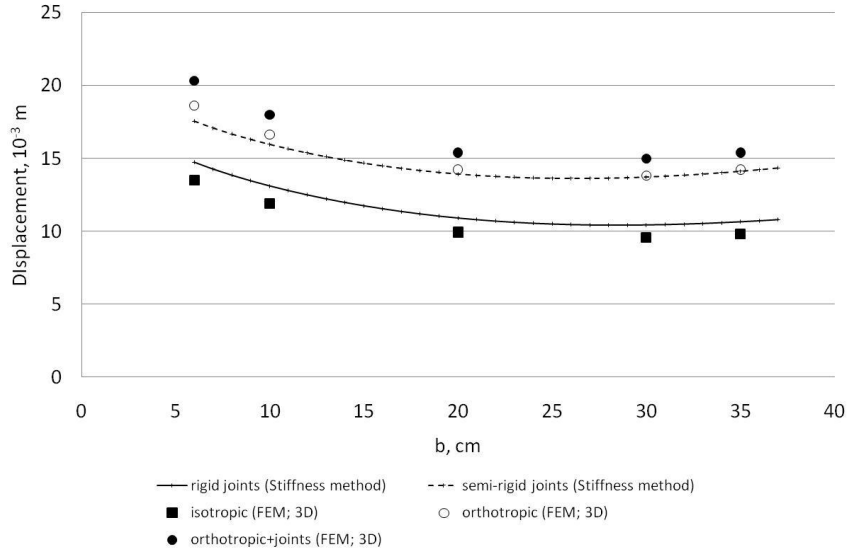

Fig. 8. Horizontal displacement of the frame top point – stretcher cross section 25,4x50,8 mm.

The results indicate that the structure becomes stiffer as the position of stretcher is lowered and/or the stretcher cross section is increased. Differences between displacement in the reference point obtained for rigid joints (matrix analysis) and isotropic model (FEM) are ranged from 6,5% (stretcher 10x20 mm) to 10% (stretcher 25,4x50,8 mm). Differences obtained for semi-rigid joints (matrix analysis) and orthotropic model with joints (FEM) are ranged from 8,5% (lower position of stretcher 25,4x50,8 mm) to 15% (upper position of stretcher 10x20 mm). It is evident, that the difference between the results obtained for isotropic model and orthotropic model with joints is largest (35% – 40%). In the case matrix analysis, the difference between displacement for structure with rigid joints and structure with semi-rigid joints is 16% - 28%.

Figure 9 shows the displacement magnitude of the chair side-frame with a stretcher, with a cross section 15x25 mm (orthotropic model with joints), at a distance between stretcher and side rail 100; 200 and 300 mm. The

stiffness of the frame increases as the position of stretcher is lowered. The increase of the stiffness can be associated with the change of the unbound length of the back leg.

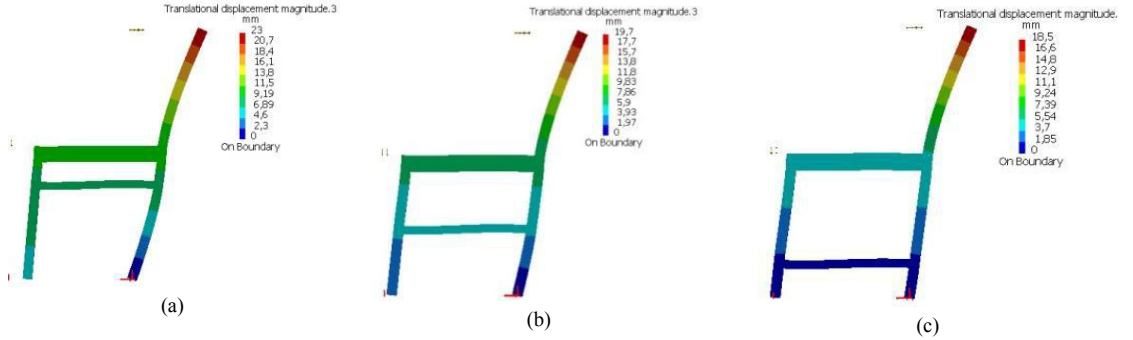

Fig. 9. Translation displacement - orthotropic model with joints: (a) b= 100 mm, (b) b=200 mm and (c) b=300 mm (scale 20:1).

Conclusion

The application of numerical method and the matrix analyses of structure in the analysis of the wood frame's structure stiffness are considered below. Similarity between the results of numerical and matrix analysis allows for the conclusion that the research models were designed correctly. The differences between results are as a consequence of method that was used, and assumptions and simplifications that were adopted. The research revealed that the numerical procedure used in the study, provides a convenient method of obtaining the information needed for determining behavior of structure. Utilization of the orthotropic mathematical model and real physical model allows efficient application of numerical method in stiffness analysis of wooden constructions. The numerical stiffness analysis and optimization of existing structure can be conducted for different and complex loading conditions. The results obtained by the direct stiffness method confirm that it can be used to achieve behavior analysis of structure in early design phase. Many variables affecting the stiffness of the structure could be quickly evaluated. The result of stiffness analysis is more realistic and reliable if joints properties i.e. semi-rigid joints are taken into consideration.

The results of numerical and matrix analyses of indeterminate wood furniture frame are also considered. Examples are given for chair's side-frame. It is evident from the analysis of the horizontal displacement of the frame's top-point that the chair's side-frame become stiffer as the position of stretcher is lowered and/or the stretcher cross section is increased. The stiffness of a furniture frame's joints has a considerable impact on the frame's deformation. More studies are needed to analyze the effect of joint-behavior on wood furniture frame.

References

[1] C.A. Eckelman, Out-of-plane strength and stiffness of dowel joints, Forest Products Journal, Vol. 29, No. 8 (1979) 32-38.
[2] P. Olsson, K.G. Olsson, Applied visualization of structural behaviour in furniture design, Chalmers University of Technology, Sweden, 2003.
[3] N. Tankut, A.N. Tankut, M. Zor, Finite element analysis of wood materials, Drvna industrija, Vol. 65, No. 2 (2014) 159-171.
[4] MH. Çolakoğlu, AC. Apay, Finite element analysis of wooden chair strength in free drop. International Journal of the Physical Sciences, (2012) 7(7): 1105−1114.
[5] S. Prekrat, N. Španić, Scientific methods for determination of wooden corner joint designs, Drvna industrija, Vol. 60, No. 4 (2009) 245-251.
[6] J. Smardzewski, Effect of wood species and glue type on contact stresses in a mortise and tenon joint, Journal of Mechanical Engineering Science, (2008) 222(12) 2293-2299.
[7] M. Derikvand, G. Ebrahimi, Finite element analysis of stress and strain distributions in mortise and loose tenon furniture joints, Journal of Forestry Research (2014) 25(3): 677−681.
[8] Y. Wanga, SH. Lee, Design and analysis on interference fit in the hardwood dowel glued joint by finite element method, 37th National Conference on Theoretical and Applied Mechanics (37th NCTAM 2013) & The 1st International Conference on Mechanics (1st ICM), Procedia Engineering, 79 (2014) 166 – 172.
[9] M. Mohamadzadeh, A. Rostampour Haftkhani, G. Ebrahimi, H. Yoshihara, Numerical and experimental failure analysis of screwed single shear joints in wood plastic composite. Materials & Design, (2012) 35: 404−413.
[10] T. J. Chung, Applied continuum mechanics, Cambridge University Press, Cambridge, 1996.
[11] J. Boding, B. A. Jayne, Mechanics of wood and wood composites, Krieger publishing Company, Malabar Florida, 1993.
[12] Y. Hsieh, Elementary theory of structures, Prentice Hall, New Jersey, 1970.

[13] S. Şeker, A. U. Öztürk, C. Kozanoğlu, Determination of reducing coefficient values of semi-rigid frames using artificial neural network, Mathematical and Computational Applications, (2011) 16 (3): 649-658.
[14] M.E. Kartal, H.B. Basaga, A. Bayraktar, M. Muvafik, Effects of semi-rigid connection on structural responses, Electronic Journal of Structural Engineering, Vol.10 (2010) 22-35.
[15] Y.Z. Erdil, A. Kasal, C.A. Eckelman, Bending moment capacity of rectangular mortise and tenon furniture joints, Forest Products Journal, Vol. 55, No. 12 (2005) 209-213.
[16] S. Hajdarevic, S. Martinovic, Effect of tenon length on flexibility of mortise and tenon joint, 24th DAAAM International Symposium on Intelligent Manufacturing and Automation, 2013., Procedia Engineering, 69 (2014) 678-685.